Journal of Applied Fluid Mechanics, Vol. 9, No. 1, pp. 303-310, 2016.
Available online at www.jafmonline.net, ISSN 1735-3572, EISSN 1735-3645.
DOI: 10.18869/acadpub.jafm.68.224.22891

Aided Mixed Convection past a Heated Square Cylinder at Low Blockage Ratio

S. Moulai[1], A. Korichi[1] and G. Polidori[2†]

[1] *LMP2M, University of Medea, Medea, Algeria*
[2] *GRESPI, University of Reims, Reims, 51100, France*

†*Corresponding Author Email: guillaume.polidori@univ-reims.fr*

(Received April 10, 2014; accepted January 17, 2015)

ABSTRACT

This paper investigates numerically the flow and heat transfer in air (Pr=0.71) by mixed convection past a heated square cylinder under aiding buoyancy effect in a confined channel. The numerical simulations are performed in the range of parameters $20 \leq Re \leq 45$ and $1.61 \times 10^3 \leq Gr \leq 6.33 \times 10^3$ for a fixed blockage ratio D/L of 0.1. The combination in the present study of these two Re and Gr parameters is reduced so that the Richarson number varies from 0,8 to 8, in order to neglect neither free convection (Ri<0.1) nor forced convection (Ri>10). The steady two-dimensional governing equations are solved by the finite volume formulation using the open source OpenFoam® code. The representative flow structure, isotherm patterns and local Nusselt number evolution are presented and discussed. The effect of both the Reynolds number and the buoyancy parameter on the fluid flow and the heat transfer are also analyzed. It is found that the wake region size strongly depends on both Reynolds and Grashof numbers and this region is shown to increase in size increasing the Reynolds number and/or decreasing the Grashof number. Moreover, increasing the Reynolds number leads to a heat transfer enhancement more pronounced on the front face of the obstacle, whereas increasing the Grashof number leads to a heat transfer enhancement more pronounced on the side faces.

Keywords: Mixed convection; Vertical channel; Heated square cylinder.

NOMENCLATURE

Cp	pressure specific heat
D	side of the square cylinder
g	acceleration due to gravity
Gr	Grashof number
H	height of channel
h	convective heat transfer coefficient
k	thermal conductivity of fluid
L	channel width
Nu	Nusselt number
P	pressure
Pe	Peclet number
Pr	Prandtl number
Re	Reynolds number
Ri	Richardson number
T	temperature
U,V	velocity components
x,y	coordinates
$I\beta$	thermal expansion coefficient
θ	no dimensional temperature
ρ	fluid density
μ	fluid dynamic viscosity
ν	fluid kinematic viscosity
0	inlet conditions
w	prism wall
$*$	dimensionless variable

1. INTRODUCTION

When flow passes over a bluff body, a near-wake takes place behind the body and a complex flow structure originates as a consequence of the mutual interactions among them.

The downstream complex flow structure originating as a consequence of the wake interactions becomes further complicated by the buoyancy effect if the free convection configuration cannot be neglected.

Many works dealing with different aspects of the heat transfer and flow behaviour over circular cylinders can be found in the literature (Zdravkovich (2003); Sumer and Fredsoe (2006). However, the flow around a square cylinder is still less investigated compared to the circular geometry, especially in the mixed convection flow regime. In literature, the steady state forced convection around a square cylinder has been investigated by Dhiman *et al* (2006). The results are presented in a large range of Prandtl number. In unsteady laminar

forced convection, the effect of channel confinement on heat transfer and fluid flow across a square cylinder has been investigated by Sharma and Eswaran (2005a). Earlier the effect of channel confinement has been carried out from both experimental and numerical investigations by Davis *et al*. (1984). The effect of Reynolds number and Prandtl number on heat transfer around a square cylinder for an unsteady flow regime is also presented by Sahu *et al*. (2009). A detailed study of the flow and heat transfer characteristics past a square cylinder in the steady and unsteady periodic flow regimes, up to a Reynolds number value of 160 and for both isothermal and constant heat flux density thermal conditions has been carried out by Sharma and Eswaran (2004a). If many experimental and numerical works devoted to forced convection heat transfer from a square cylinder can be found in the literature, much less attention has been devoted to mixed convection and particularly to heat transfer features. When the buoyant forces are imparted over the viscous phenomenon, the flow behind the cylinder becomes more complicated as a result of interactions between viscous and buoyancy forces. The flows are endowed with strong interactions that can complicate the heat transfer process, especially when free and forced convection effects are comparable.

In pure free convection, Saha (2000) investigated the phenomena past a square cylinder placed centrally within a vertical parallel plate channel. The flow was found unstable above the critical Grashof number $Gr = 3 \times 10^4$. The author found that the drag coefficient decreases while the Strouhal number increases with increasing Grashof number. Khodary and Bhattacharyya (2006) studied natural convection from a horizontal isothermal square cylinder inside a vertical adiabatic channel. Theirs results indicate that the laminar natural convection is significantly affected by the aspect ratio and the lateral position of the obstacle. Whatever the Grashof number is, an optimum aspect ratio exists, leading to the maximum heat transfer rate. Central positioning is observed to be the best way to enhance the heat transfer.

In steady state mixed convection regime, Dhiman el al. (2008) studied the effect of cross-buoyancy and Prandtl number on the flow and heat transfer characteristics of an isothermal confined square cylinder in a channel. The drag coefficient was found to be less sensitive to the Richardson number than the lift coefficient. The influence of the Richardson number on the total drag coefficient and the Nusselt Number is qualitatively similar to the case of the unconfined mixed convection. The value of Nusselt number was found to increase up to 5% compared to the pure forced convection value.

One of the first numerical study on the cross buoyancy effect in confined channel has been investigated by Biswas *et al*. (1990). They reported that the maxima and minima in the velocity and temperature profiles were found close to the bottom walls of the channel. They also reported that the periodicity of flow and asymmetry of the wake can occur at lower Reynolds numbers in the same manner as pure forced convection.

Suzuki and Suzuki (1994) reported numerical and experimental studies on the confined flow obstructed by a square cylinder maintained at constant temperature at Re = 50, 100 and 150 under various inlet flow conditions. From the numerical results, the flow was found to fluctuate in a highly periodic fashion and the Karman vortex formed downstream from the rod exhibited a crisscross motion in the obstructed channel flow. Turki *et al*. (2003b) have numerically investigated the mixed convection from a horizontal square cylinder in air for Re=120 to 200, for Ri up to 0.1 at a blockage ratio of 0.25 and 0.125. The critical value of Reynolds number was observed to increase with increasing the blockage ratio in pure forced convection. In mixed convection, the critical Reynolds number was found to decrease with increasing Richardson number while the Strouhal number was reported to increase with Richardson number.

Sharma and Eswaran (2004a), studied numerically the heat and fluid flow across a square cylinder at Reynolds number of 100 under aiding and opposing buoyancy. They found that the degeneration of Karman Vortex Street occurs at a critical Richardson number of 0.15. Also, they notified that the average Nusselt number for the cylinder increases monotonically with the Richardson number, albeit only slightly. In another study by Sharma and Eswaran (2005b), the same authors has investigated the aiding/opposing buoyancy for $-1 \leq Ri \leq 1$ around a confined square cylinder in a channel for the varying values of blockage ratio at the constant value of Reynolds number of 100 and Prandtl number of 0.7. They reported that the minimum heating (critical Ri) required for the suppression of vortex shedding decreases up to a certain blockage ratio (=30%), but thereafter increases with increasing the blockage ratio for the flow around a square cylinder. They also found that the cylinder Nusselt number increases with increasing the blockage ratio and Ri.

Bhattacharyya and Mahapatra (2005) studied the influence of buoyancy on the vortex shedding and heat transfer from a cylinder of square cross-section exposed to a horizontal stream for a wide range of Re (up to 1400) with Ri = 0-1 and Pr = 0.72. They showed that the vortex shedding behind the cylinder takes place for a Reynolds number greater than 40 over the entire range of Richardson number considered. Also, their results showed that the centerline symmetry of the wake is lost and the cylinder experiences a downwards lift when the buoyancy effect is considered. Perng and Wu (2007) investigated the aiding/opposing buoyancy on turbulent heat transfer for $-1 \leq Ri \leq 1$. They conclude that with increasing the blockage ratio, the buoyancy effect is becoming weaker on the Nusselt number for the square cylinder.

From an experimental investigation, Singh *et al*. (2007) studied the effect of aiding buoyancy on the wakes of circular and square cylinders at low

Reynolds numbers. They observed that the critical Richardson number increases with Reynolds number. Also, they found that the critical *Ri* for a square cylinder is close to that of a circular cylinder at comparable *Re*.

Using the Schlieren technique, a detailed investigation of the effect of buoyancy and incidence angle on the vortex shedding process has been carried out by Kakade *et al*. (2010).

They observed that buoyancy delivers sufficient momentum into the wake, diminishes the velocity deficit, and completely eliminates the vortex shedding at a critical Richardson number that depends on the Reynolds number and the angle of incidence. Moreover, for a given orientation, Strouhal number is found to be a function of both the Reynolds number and the Richardson number. With an increase in Richardson number, the Strouhal number increases owing to the aiding buoyancy force. However, vortex shedding abruptly ceases at and beyond a certain critical Richardson number. The effects of cross buoyancy on vortex shedding behind a square cylinder in 2D laminar flow regime have been investigated by Chatterjee and Mondal (2011) for 5 ≤*Re*≤40 and 0≤*Ri*≤2. The thermal buoyancy brings about asymmetry in the wake and induces unsteadiness beyond some critical value of Richardson number for a particular Reynolds number. The critical Richardson number for the onset of vortex shedding is found to decrease with increasing *Re*. The shedding frequency increases with *Re* and *Ri* beyond its critical value.

Recently, Sharma *et al*. (2012) performed numerical simulations of aiding mixed convection across a square cylinder at low Reynolds numbers (0 – 40). They found that the flow is still steady for the range of conditions taken in the study. The friction drag, pressure drag and total drag coefficients decrease with increasing Reynolds number; whereas, the opposite trend is observed with increasing Richardson number. The average Nusselt number increases with Reynolds number and/or Richardson number.

Thus, based on the previous review, it clearly appears a lack of studies that have dealt with aiding buoyancy over a square cylinder in the vertical channel. The few of them who were still on this topic focused on the onset/breakdown of Karman vortex street cylinder wakes. Accordingly, there is a need for further studies in heat transfer and fluid flow at low Reynolds number under the buoyancy aided regime. It is the reason why the purpose of the present work is to study heat transfer and fluid flow around a square cylinder at Reynolds numbers 20≤Re≤ 45 and Richardson number, 0.5≤Ri≤ 10 for air (Pr=0.71).

2. MODELLING

The two-dimensional physical geometry and the relevant dimensions considered for the numerical analysis are schematically shown in Fig 1. In the present numerical investigation, the flow is assumed to be steady, laminar and two-dimensional in the range of parameters used. Indeed, for a confined channel with a blockage ratio equal to 1/8 (close to the configuration of the present study), Turki *et al*. (2003a) found a critical Re value of 62 from steady to periodic motion. This value is confirmed by an experimental investigation for unconfined flow by Kakade *et al*. (2010) where the authors found a critical Re of 56. In a previous study by Korichi *et al*. (2005) and Korichi and Oufer (2007)), for a pure forced convection in similar configuration, the critical Re was found about 60. Moreover, the transition to three-dimensionality is found to take place at a Reynolds number between 150 and 175 (Saha *et al*., (2000, 2003a, 20003b); Luo *et al*. (2003); Xiaohu (2003) and Gregory *et al*. [30]). Also, from only the buoyancy effect view, unsteady and three-dimensionality of the flow may occur for high Grashof numbers outside the investigated range (Atmane *et al*., (2003)).

The incompressible Navier–Stokes and energy equations in the Cartesian coordinate system form the governing equations of the flow. The buoyancy-driven flow from the heated surface interacts with the laminar main flow to yield mixed convection conditions. Viscous dissipation is neglected and constant thermophysical properties of the medium are assumed, except the density where Boussinesq approximation is used to estimate the thermal buoyancy term in momentum equation.

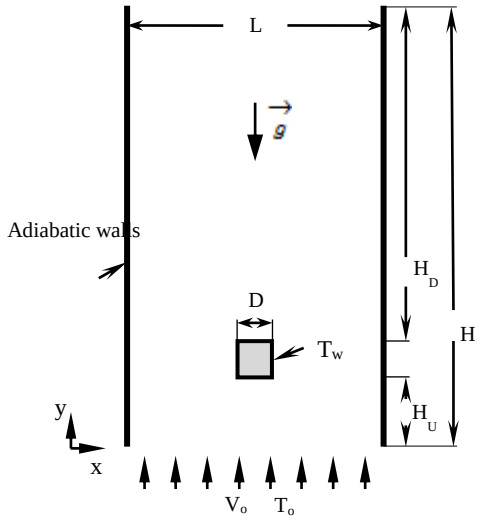

Fig. 1. Physical configuration of the problem.

Thus, the continuity, the x and y components of the Navier-Stokes and the energy equation in the nondimensional form can be written as follow:

$$\frac{\partial u^*}{\partial x^*} + \frac{\partial v^*}{\partial y^*} = 0 \tag{1}$$

$$u^* \frac{\partial u^*}{\partial x^*} + v^* \frac{\partial u^*}{\partial y^*} = -\frac{\partial p^*}{\partial x^*} + \frac{1}{\mathrm{Re}}\left(\frac{\partial^2 u^*}{\partial x^{*2}} + \frac{\partial^2 u^*}{\partial y^{*2}}\right) \tag{2}$$

$$u^* \frac{\partial v^*}{\partial x^*} + v^* \frac{\partial v^*}{\partial y^*} = -\frac{\partial p^*}{\partial x^*} + \frac{1}{\mathrm{Re}}\left(\frac{\partial^2 v^*}{\partial x^{*2}} + \frac{\partial^2 v^*}{\partial y^{*2}}\right) + Ri\theta^* \tag{3}$$

$$u^* \frac{\partial \theta^*}{\partial x^*} + v^* \frac{\partial \theta^*}{\partial y^*} = \frac{1}{Pe}\left(\frac{\partial^2 \theta^*}{\partial x^{*2}} + \frac{\partial^2 \theta^*}{\partial y^{*2}}\right) \quad (4)$$

Where the dimensionless variables are defined as:

$$x^* = \frac{x}{H}, \quad y^* = \frac{y}{H}, \quad u^* = \frac{u}{v_0}, \quad v^* = \frac{v}{v_0},$$

$$p^* = \frac{p}{\rho . v_0^2} \quad \theta^* = \frac{T - T_0}{T_w - T_0} \quad (5)$$

The Reynolds number, Grashof number, Richardson number, Peclet number and Prandtl number represent physically, the ratios of inertial to viscous forces, buoyancy to viscous forces, advection to diffusion rates and momentum to thermal diffusivities. These numbers correspond to the governing phenomena parameters for this problem and are respectively defined as

$$\mathrm{Re} = \frac{\rho v_0 D}{\mu}, \; Gr = \frac{g\beta D^3 (T_w - T_0)}{\nu^2},$$

$$Ri = \frac{Gr}{\mathrm{Re}^2}, \; Pe = \mathrm{Re}.\mathrm{Pr} \quad (6a)$$

Where

$$\text{and } \mathrm{Pr} = \frac{\mu C_p}{k} \quad (6b)$$

The boundary conditions of interest in this study are as follows:

At the inlet a uniform upward flow of constant temperature is prescribed

$$u^* = 0 \;,\; v^* = 1,\; \theta^* = 0 \quad (7a)$$

At the outlet, an outflow boundary condition is given:

$$\frac{\partial u^*}{\partial y^*} = 0, v^* = 0, \frac{\partial p^*}{\partial x^*} = 0, \; \frac{\partial \theta^*}{\partial y^*} = 0 \quad (7b)$$

The boundary conditions on the cylinder surface are given by:

$$u^* = 0 \;,\; v^* = 0 \;,\; \theta^* = 1 \quad (7c)$$

Finally, ‘‘no-slip’’ boundary conditions are applied to the two adiabatic channel walls:

$$u^* = 0, \; v^* = 0, \frac{\partial \theta^*}{\partial x^*} = 0 \quad (7d)$$

3. NUMERCICAL METHOD

The governing transport equations associated with the boundary conditions are solved using the open source OpenFoam® code (2011) based on the finite volume formulation. The *buoyant Boussinesq Simple Foam* solver is employed ; it is based on the SIMPLE algorithm and uses the Boussinesq approximation for estimating the density in buoyancy term in the momentum equation.

The grid is chosen non uniform and is highly concentrated close to the square cylinder to capture high gradient velocity, pressure and temperature. In order to ensure a grid independence for the results, a series of tests for non uniform grids were carried out. The nodes are equally spaced on the cylinder edges, whereas an adequate expansion ratio characterizes the node distribution on the other edges of the domain. Mesh grid distribution which corresponds to an interval grid size on the surface on cylinder of $1.67\ 10^{-4}$ was found sufficient to produce independent results. The maximum relative error for global parameters such as mean *Nusselt* number not exceeds 2% for Re= 45 and Gr= 3216. The effect of upstream and downstream distances on the physical parameters has been examined in previous studies for a similar configuration (Korichi el al. (2005), Korichi and Oufer (2005, 2007) at greater Reynolds numbers. Analysis showed that, under the conditions taken in the present study, the following distance values were still applicable. Consequently, an upstream distance L_u = 6.0 from the domain edge to the face of the obstacle and a downstream distance L_D = 23 were found sufficient to have no effect on the results.

Validation of the numerical simulation was attained by performing comparisons with previous works. Indeed, Fig. 2 shows the results of the present work compared with those of Dhiman *et al*. (2006) for the same conditions. A quite good agreement is observed between the two studies and the maximum relative error is within 4%.

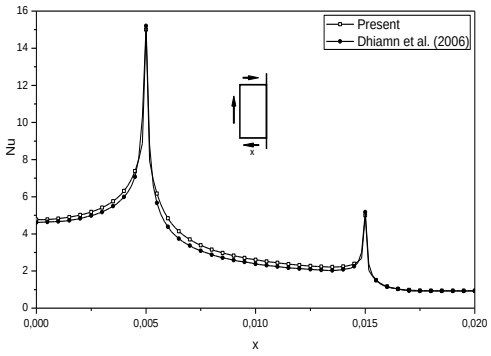

Fig. 2. Validation plot of the present numerical simulation by comparison with the results.

4. DISCUSSION

In this study, numerical computations have been carried out for $20 \leq Re \leq 45$ and $1.61x10^3 \leq Gr \leq 6.33x10^3$ corresponding varying from Ri=0.8 to 8. This parameter range was chosen, because both free and forced heat transfer affect the flow which remains in the steady state conditions. Prandtl number of the fluid is taken equal to 0.71 (air) and the blockage ratio considered in this study is chosen constant and equal to 1/10.

4.1 Flow structure and isotherm patterns

Figure 3 shows the streamlines contours in the

vicinity of the square cylinder for Re=20, 30 and 45 and Gr=3.22x10^3 respectively, corresponding to Ri varying from 8.0 to 1.6. One can easily distinguish a closed steady recirculating area taking place from the fixed trailing edges of the square cylinder composed by two counter-rotating and symmetric small vortices. In front of the cylinder a separation of the flow occurs and a stagnation point is formed. Because the upstream flow. Since the upstream flow is relatively low, no separation occurs from the two corners of the leading face of the square cylinder. Then, since only the sharp trailing corners of the square cylinder fix the points of separation in the range of Re considered in this study, it can be easily seen that the length of the recirculation region increases with increasing Reynolds number. More details of the wake geometry will be further presented. It should also be noted that the flow structure remains still symmetric under the conditions of this study.

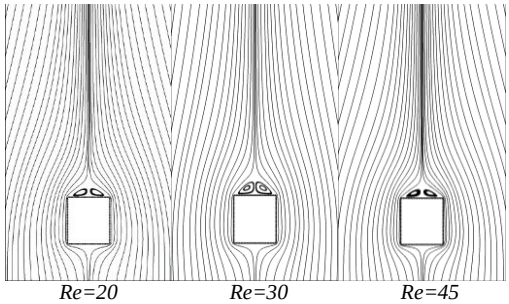

Re=20 *Re=30* *Re=45*

Fig. 3. Streamlines contours for Re=20, 30 and 45 at Gr=3.22 10^3.

The isotherm maps in the vicinity of the square cylinder are shown in fig. 4 for the same parameter values, namely Re=20, 30 and 45 and Gr=3.22x10^3. Under aided buoyancy effect, the isotherms follow the main flow structure and present also a symmetric behaviour from the mid-line of the flow. From these maps, it can be seen that the isotherms are congregated at the front stagnation region, signifying the highest heat transfer rate from the cylinder surface in this region as compared to the rear and the side surfaces. Similar findings are reported for the pure forced convection case for a square cylinder (Sahu *et al*. (2009)) as well as for a circular cylinder (Sarkar *et al*. (2011)). From the isotherm maps, it can be concluded that the thermal boundary layer on the front face is the thinnest followed by the one on the side faces and at least by the plume on the rear face. Obviously, it can be seen a similarity between the wake and the thermal plume shape.

In the wake region, where a recalculating zone exists, the isotherms are widely spread and are closely packed for the shorter recirculation region. Because, the amount of fluid in the recirculation zone increases with increasing Reynolds number, the clustering of isotherms also increases with increasing the Reynolds number. The temperature contours spread along the streamwise direction with a subsequent reduction of the lateral width. The main difference between the pure forced convection and the buoyancy aided mixed convection is that the isotherms show a thin plume rising in the far field above from the heated cylinder. The thermal boundary layer starts from the front corner of the side face and growth as the flow moves towards in the streamwise direction. Another difference as compared to the pure forced convection is that the thermal boundary layer thickness in the mixed convection case is lower for a same Reynolds number, except at the front face for high Grashof number.

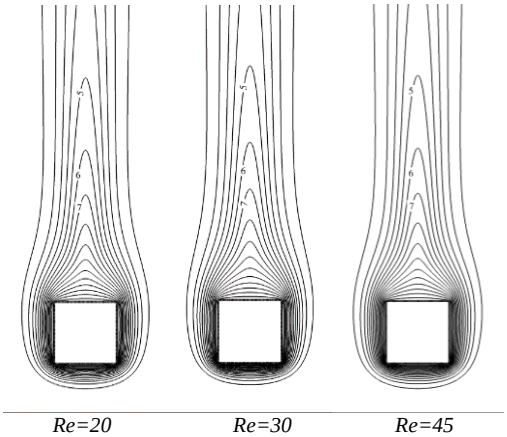

Re=20 *Re=30* *Re=45*

Fig. 4. Isotherm contours for different Re at Gr=3.22 10^3.

The local Nusselt number evolution the along the half peripheral cylinder surfaces for various Reynolds number at Gr=3.22x10^3 is depicted in fig. 5.

As expected, for reason of symmetry, Nusselt number is presented only for a half perimeter as indicated in figure legend. The Nusselt number along the front face presents the highest evolution compared to the other faces of the cylinder. Starting from the flow stagnation point, situated on the middle of the front face, Nu increases quite sharply along the frontal face until peak values are attained at the first corner, whatever the Reynolds number is. On the side face, Nu decreases along the flow direction as the heat flux in the upstream is convected downwards by the fluid.

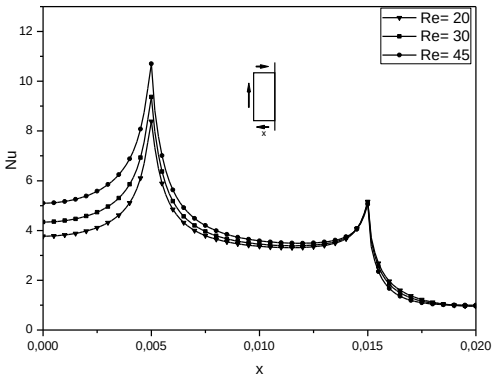

Fig. 5. Local Nusselt number evolution along one half of the cylinder surfaces for various Reynolds number at Gr=3.22.10^3.

On the rear face, the *Nusselt* number falls considerably to reach values below those observed for the other faces. This is due to the effect of the diffusive heat transfer mode which is non negligible compared to the convective mode in the wake where the rear face is in contact with the two vortices. It can be clearly observed that values of the Nusselt number become higher with increasing values in the Reynolds number except along the rear face, as expected the diffusion is the main heat transfer mode. It should be noted that although the front face is in contact with the unheated free air stream, the Nusselt number is very low in the middle of the face due to the presence of the stagnation point which divides the flow into two. The effect of Reynolds number is more pronounced on the front face, which is the direct target of the incoming free stream flow.

The mean Nusselt number for each face of the square cylinder is calculated by averaging the local Nusselt number over the cylinder surfaces for each Reynolds number value. The results are shown in fig. 6.

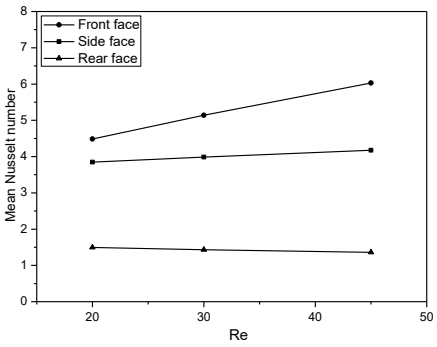

Fig. 6. Mean *Nusselt* number by face for various Reynolds number at Gr=3.22.10^3.

Increasing the Reynolds number from 20 to 30 leads to an increase of the Nusselt number of about 13% and 3.20% for the front and the side faces respectively. However a decrease of 4.3% is observed for the rear face. The reason is that, at relatively low Richardson number, the warm fluid is imprisoned trapped in the recirculating wake leading to reduce the heat transfer. Similar results are also observed for Reynolds number varying from 30 to 45. The analysis of mixed convection is more complicated than that of the pure forced or free convection only. To get a better understanding of this phenomenon, the influence of buoyancy on the fluid flow and thermal field around the square cylinder is shown by plotting the streamlines and isotherms contours for different Grashof number values in fig. 7 and fig. 8, respectively.

The heat released from the cylinder surface decreases the fluid density in the prism vicinity and consequently the fluid will start to move in the direction opposite to the gravity, and this motion will be added to the upward inertial flow. The combination of these two motions tends to accelerate the boundary layer flow in the vicinity of the heated square cylinder. When the buoyancy forces are conjugated over the viscous phenomenon, the induced flow moves upward making a kind of smooth turn around the hot square cylinder. As the Grashof number increases, the boundary layer induced by the upward buoyancy flow is found to be more accelerated and becomes finer. At a fixed Reynolds number value, increasing the Grashof number results in reducing the recirculating zone size behind the square cylinder. This can be explained by the elevation of the temperature, so that vortices formed in the wake are weakened by the buoyancy force due to the decrease of the fluid density in the vicinity of the cylinder.

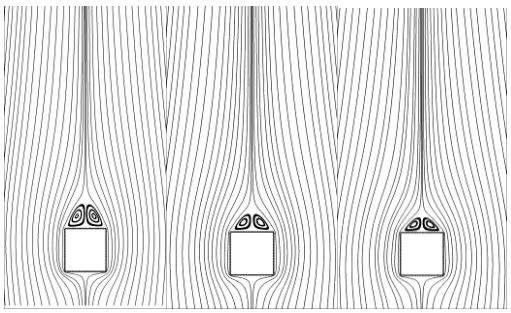

Fig. 7. Streamline contours for different Grashof numbers at Re=45.

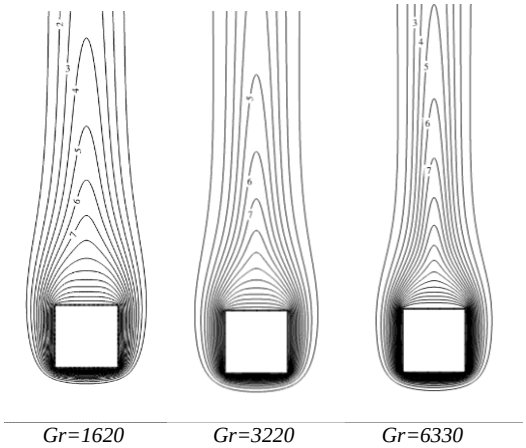

Fig. 8. Isotherm contours for different Grashof numbers at Re=45.

The effect of Grashof number on the local Nusselt number evolution along the half cylinder peripheral surface at Re=45 is shown in fig. 9. It can be seen that the increase of the cylinder temperature surface leads to an increase of the Nusselt number on the lateral side face followed by a slight increase on the rear face. However, no significant effect is observed on the front face. This effect is opposite to that observed with increasing the Reynolds number. This result can be explained as follow: due to the increase in heating amount, the buoyancy effect accelerates the flow in the vicinity of the side faces and the heat removed by free convection is added to the forced convection.

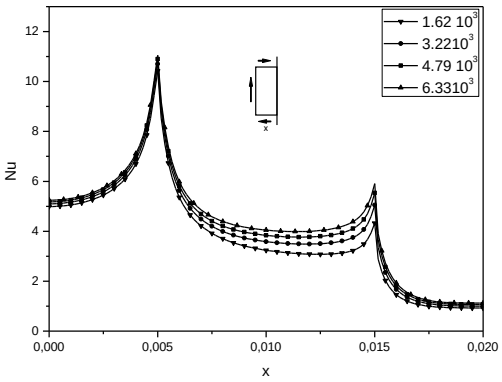

Fig. 9. Local Nusselt number evolution along one half of the cylinder surfaces for various Grashof number at Re=45.

For the front face, as increasing the buoyancy parameter of the thermal boundary layer thickness as a result of the free flow which tends to leave the heated surface. Figure 10 shows the mean Nusselt number by face for different Grashof numbers at Re=45.

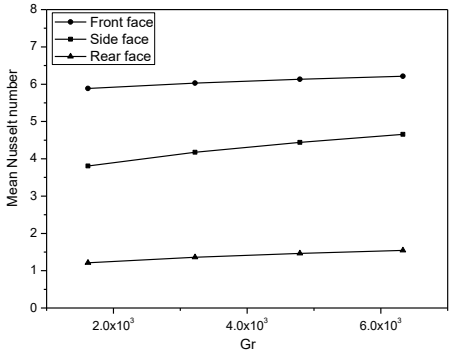

Fig. 10. Mean *Nusselt* number by face for various Grashof number at Re=45.

5. CONCLUSION

A numerical study of two-dimensional flow and heat transfer past a horizontal square cylinder under buoyancy aided effect has been reported, for the steady state conditions. The effect of the Reynolds number ($20 \leq Re \leq 45$) and the Richardson number ($0.8 \leq Ri \leq 8$) on the flow and heat transfer are investigated. The blockage ratio and Prandtl number are taken constant and equal to 0.1 and 0.7 (air), respectively. The results show that in steady state conditions, both streamlines and isotherms are symmetric about the centerline upstream as well as in the wake region of the square cylinder. The isotherms contours are congregated at the front region, leading to the highest heat transfer rate from the cylinder surface in this region as compared to the other sides. Moreover, heat transfer is the lowest at the rear surface. It is found that the size of the wake region increases with increasing the Reynolds number and reduces in size with increasing the Grashof number. It is noticed that the augmentation of the Reynolds number leads to an increase in the Nusselt number on the front side while the augmentation of the Grashof number increases the Nusselt number on the lateral faces.

REFERENCES

Atmane, M. A., V. S. S. Chan and D. B. Murray (2003). Natural convection around a horizontal heated cylinder: The effects of vertical confinement. *International Journal of Heat and Mass Transfer* 46, 3661–3672.

Bhattacharyya, S. and S. Mahapatra (2005). Vortex shedding around a heated square cylinder under the influence of buoyancy. *Heat and Mass Transfer* 41, 824–833.

Biswas, B., H. Laschefski, N. K. Mitra and M. Fiebig (1990). Numerical investigation of mixed convection heat transfer in a horizontal channel with built-in square cylinder. *Numerical Heat Transfer Part A* 18(2), 73–188.

Chatterjee, D. and B. Mondal (2011). Effect of thermal buoyancy on vortex shedding behind a square cylinder in cross flow at low Reynolds numbers. *International Journal of Heat and Mass Transfer* 54, 5262–5274.

Davis, R. W., E. F. Moore and L. P. Purtell (1984). A numerical-experimental study of confined flow around rectangular cylinders. *Physics of Fluids* 27(1), 46-59.

Dhiman, A. K., R. P. Chhabra and V. Eswaran (2008). Steady mixed convection across a confined square cylinder. *International Communications in Heat and Mass Transfer* 35, 47–55.

Dhiman, A. K.**,** R. P. Chhabra, A. Sharma and V. Eswaran (2006). Effects of Reynolds and Prandtl Numbers on Heat Transfer Across a Square Cylinder in the Steady Flow Regime. *Numerical Heat Transfer Part A* 49(7), 717 – 731.

Kakade, A. A., S. K. Singh, P. K. Panigrahi and K. Muralidhar (2010). Schlieren investigation of the square cylinder wake: Joint influence of buoyancy and orientation. *Physics of Fluids*. 22, 054107, 1-18.

Khodary, K. and T. K. Bhattacharyya (2006). Optimum natural convection from square cylinder in a vertical channel. *International Journal of Heat and Fluid Flow* 27, 167–180.

Korichi, A., H. Chérifi and L. Oufer (2005) Transfert convectif lors d'un écoulement oscillatoire en présence d'un barreau cylindrique, *17ème congrès français de Mécanique -Troyes, France.*

Korichi, A. and L. Oufer (2007). Etude numérique de l'écoulement instationnaire et du transfert de

chaleur autour d'une conduite de section carrée dans un canal. *Science et Technologie A* 25, 55-61.

Korichi, A. and L. Oufer (2005). Numerical heat transfer in a rectangular channel with mounted obstacles on the upper and lower walls. *International Journal of Thermal Sciences* 44(7), 644–655.

Luo, S. C., Y. T. Chew and Y. T. Ng (2003). Characteristics of square cylinder wake transition flows. *Physics of Fluids* 15(9), 2549-2559.

OpenCFD L. t. d. (2011). *OpenFOAM - The Open Source CFD Toolbox*, Version 2.0.0

Perng, S. W. and H. W. Wu (2007). Buoyancy-aided/opposed convection heat transfer for unsteady turbulent flow across a square cylinder in a vertical channel. *International Journal of Heat and Mass Transfer* 50, 3701–3717.

Saha, A. K. (2000). Unsteady free convection in a vertical channel with a built-in heated square cylinder. *Numerical Heat Transfer A*. 38(8), 795–818.

Saha, A. K., K. Muralidhar and B. Biswas (2003a). Investigation of Two- and Three-Dimensional Models of Transitional Flow Past a Square Cylinder. *Journal of Engineering Mechanics* 129(11), 1320-1329.

Saha, A. K., G. Biswas and K. Muralidhar (2003b). Three-dimensional study of flow past a square cylinder at low Reynolds numbers. *International Journal of Heat and Fluid Flow* 24, 54–66

Saha, A. K., K. Muralidhar and G. Biswas (2000). Transition and chaos in two-dimensional flow past a square cylinder. *Journal of Engineering Mechanics* 126(5), 523-532.

Sahu, A. K., R. P. Chhabra and V. Eswaran (2009). Effects of Reynolds and Prandtl numbers on heat transfer from a square cylinder in the unsteady flow regime. *International Journal of Heat and Mass Transfer* 52, 839–850.

Sarkar, S., A. Dalal and G. Biswas (2011). Unsteady wake dynamics and heat transfer in forced and mixed convection past a circular cylinder in cross flow for high Prandtl numbers. *International Journal of Heat and Mass Transfer* 54, 3536-3551.

Sharma, N., A. K. Dhiman and S. Kumar (2012). Mixed convection flow and heat transfer across a square cylinder under the influence of aiding buoyancy at low Reynolds numbers. *International Journal of Heat and Mass Transfer* 55, 2601–2614.

Sharma, A. and V. Eswaran (2005a). Effect of Channel-Confinement on the Two-Dimensional Laminar Flow and Heat Transfer across a Square Cylinder. *Numerical Heat Transfer A* 47(1), 79-107.

Sharma, A. and V. Eswaran (2005b) Effect of channel-confinement and aiding/opposing buoyancy on the two-dimensional laminar flow and heat transfer across a square cylinder. *International Journal of Heat and Mass Transfer* 48, 5310–5322.

Sharma, A. and V. Eswaran (2004a). Effect of aiding and opposing buoyancy on the heat and fluid flow across a square cylinder at Re = 100. *Numerical Heat Transfer, Part A* 45(6), 601–624.

Sharma, A. and V. Eswaran (2004b). Heat and fluid flow across a square cylinder in the twodimensional laminar flow regime. *Numerical Heat Transfer A* 45(3), 247-269.

Sheard, G. J., M. J. Fitzgerald and K. Ryan (2009). Cylinders with square cross-section: wake instabilities with incidence angle variation. *Journal of Fluids Mechanics* 60, 43–69.

Singh, S. K., P. K. Panigrahi and K. Murlidhar (2007). Effect of buoyancy on the wakes of circular and square cylinders: a schlieren-interferometric study. *Experiments in Fluids* 43, 101–123

Sumer B. M. and J. Fredsoe (2006). *Hydrodynamics around cylindrical structures*. World Scientific Publishing, London.

Suzuki K. and H. Suzuki (1994). Unsteady heat transfer in a channel obstructed by an immersed body. *Annual Review of Heat Transfer* C. L. Tien (Ed.) 5, 177–206.

Turki, S., H. Abassi and S. Ben Nasrallah (2003a). Effect of the blockage ratio on the flow in a channel with a built-in square cylinder. *Computational Mechanics* 33, 22-29

Turki, S., H. Abbassi and S. Ben Nasrallah (2003b). Two-dimensional laminar fluid flow and heat transfer in a channel with a built-in heated square cylinder. *International Journal of Thermal Sciences* 42, 1105–1113

Zdravkovich, M. M. (2003). *Flow around circular cylinders* 2 Applications. Oxford University Press, Oxford.

Xiaohu, T. (2003). *Transition phenomena in the wakes of cylinders*, PhD thesis, National university of Singapore.